

Defining a sample heterogeneity cut-off value to obtain representative Special Core Analysis (SCAL) measurements

Jos G. Maas ^{1,*}, Niels Springer ², and Albert Hebing ¹

¹PanTerra Geoconsultants BV, Weversbaan 1-3, 2352 BZ Leiderdorp, The Netherlands

²GEUS, Øster Voldgade 10, 1350 København, Denmark

Abstract. Recently we published a method to quantitatively assess a heterogeneity number V that indicates the variability of the absolute permeability in a core plug. At that time, however, we could not provide a suitable cut-off for V . Therefore, the risk remained that SCAL measurements could be conducted on samples with a local distortion dominating flow and water cut behaviour. Subsequent use of the extracted relative permeability data in a reservoir simulation model would cause the field behaviour to be dominated in the same way, generating significantly wrong forecasts. In the present study, more than 70 scenarios for synthetic heterogeneous core plugs were simulated to study the impact of heterogeneity onto flow parameters measured in SCAL experiments. Both Unsteady-State and Centrifuge experiments on these synthetic plugs were simulated in 3-D. Subsequently, the simulated production data were history matched with a newly developed AutoSCORES software package to extract the relative permeability and capillary pressure in an objective manner. A rigorous statistical analysis was applied to determine a cut-off value for the heterogeneity number V for each listed scenario. The cut-off proved to be strongly dependent on the number of samples available in a SCAL study. First experimental results of measurements on actual rock samples are in line with predictions. A table is presented to assist SCAL experimentalists in deciding which SCAL samples reliably can be used for a SCAL study unaffected by the effects of heterogeneities, based on V of a sample.

1 Introduction

Special Core Analysis (SCAL) data are used as input in reservoir simulation models to predict long term oil and gas field behaviour as part of field development planning. State-of-the-art interpretation-by-simulation of the data, as well as conventional analytical data analysis (e.g. “JBN” [1], “Hassler-Brunner” [2]) requires the core plugs to be homogeneous. Today, no industry accepted methods exist to deal with heterogeneous plugs, while the common belief is that hardly any core plug is perfectly homogeneous.

A serious problem develops when SCAL measurements are conducted on core plugs with a local distortion dominating flow and water cut behaviour. Subsequent use of the extracted relative permeability data in a reservoir simulation model would cause the field behaviour to be dominated in the same way, generating significantly wrong forecasts. The problem was addressed by several authors already many years ago [3, 4, 5], but only qualitative results were presented in the absence of a heterogeneity number at the time.

Building on earlier work where we identified a heterogeneity number V [6], we now have conducted a detailed study into the effect of various possible heterogeneity scenarios onto measured relative permeability, such as stochastically distributed heterogeneities throughout the whole plug, a thin high-

permeability zone, etc. We used SCORES3D (a 3D version of license-free SCAL simulator SCORES [7, 8]), to study in total more than 70 synthetic scenarios, covering what we believe are typical heterogeneity occurrences in core plugs.

The paper first discusses the general design of the study, clarifying the necessity to follow primarily a simulation approach. Subsequently, the heterogeneity scenarios are presented, followed by a discussion of the automatic history matching tool AutoSCORES we developed to achieve objective evaluations of the relative permeabilities impacted by the heterogeneities.

Central to the work is the interpretation of the results following a rigorous statistical analysis. This is explained in detail in a separate Section.

Finally, laboratory SCAL experiments are presented that were conducted in support of the analysis of the simulation study.

2 General design of the study

We will first present the outline for the study in determining a cut-off value for heterogeneity number V as it could happen in an ideal world where no budget or time restrictions play a role. Subsequently, we show how from this ideal study program we derived the workflow followed in this study.

* Corresponding author: jgmaas@euronet.nl

2.1 Ideal approach studying effect of heterogeneity on SCAL measurements on core plugs

In an ideal, unconstrained world one could set up a measurement program with the following steps:

1. Identify a base case set of perfectly homogeneous samples, i.e. samples with $V=0$. The heterogeneity number V is defined in our earlier paper [6] as

$$V = \frac{d}{a} \sigma_{HU} \quad (1)$$

with d determined from an exponential correlation between porosity and permeability from routine core analysis (RCA) data and parameter a determined from a linear correlation between porosity and Hounsfield numbers from CT-images of the plugs. σ_{HU} is the standard deviation of the Hounsfield values in the CT-image of the plug.

To improve the statistical accuracy of the selection, the set should consist of at least 10 plugs, preferably 100 or more plugs (see Section 5).

2. Collect samples with increasing V numbers and of different topologies (i.e. layered, or containing impermeable spots or streak, open vugs, etc.). At least 10, preferably 100 samples or more per chosen V and chosen topology are required for reliable statistics (see Section 5).
3. Conduct RCA on all samples for porosity ϕ and absolute permeability K .
4. Conduct CT scanning on all samples to assess the individual V numbers, using Eq. 1.
5. Restore wettability through aging at representative initial water saturation and conduct imbibition SCAL experiments on all samples with a combination of UnSteady-State (USS) for relative permeability and Multispeed Centrifuge measurements for capillary pressure. Note that although SCAL data are primarily used to determine relative permeabilities, the capillary pressure function needs to be determined to be able to account properly for end-effects in the measurements.
6. Extract the water relative permeability k_{rw} , oil relative permeability k_{ro} and capillary pressure P_c using an interpretation-by-simulation technique.
7. Determine the cut-off value for V , beyond which the extracted relative permeabilities are found to be significantly different from the homogeneous base case, using sample statistics.

Clearly, the above approach is impossible to carry out because of practical limitations in time and budget.

2.2 Approach followed in this study

We have chosen to use synthetic core plugs constructed in software rather than real rock. The software employed is a newly developed extension into 3 dimensions of the license-free SCAL simulator SCORES built on DuMux [7, 8]. Simulations were conducted on a grid of 16 x 16 x 50 grid blocks. The capabilities of SCORES3D are described in Section 4. Our workflow has been set-up staying close to the ideal approach discussed above:

1. A homogeneous base case was defined as a core plug with $K=10$ mD, and $\phi=0.17$.

Relative permeabilities were defined using the Corey parameters listed in Table 1. We use the following Corey formulations for the water and oil relative permeabilities k_{rw} and k_{ro} respectively:

$$k_{rw}(S_w) = k_{rwor} \left(\frac{S_w - S_{wc}}{1 - S_{wc} - S_{or}} \right)^{n_w} \quad (2)$$

$$k_{ro}(S_w) = k_{rowc} \left(\frac{1 - S_w - S_{or}}{1 - S_{wc} - S_{or}} \right)^{n_o} \quad (3)$$

A capillary pressure function $P_c(S_w)$ was constructed similar to case 0, as used by Reed and Maas [9] (see also Gupta and Maloney [10]).

2. A range of heterogeneity scenarios was built with SCORES3D, based on experience in the laboratory. In total more than 70 heterogeneous plugs were constructed in software. Details of the scenarios are described in Section 3.
3. RCA is replaced by a numerical approach to calculate the effective K and ϕ for each synthetic plug.
4. CT scans are replaced by numerical calculation of V for each scenario, i.e. each individual synthetic plug.
5. SCAL is replaced by simulation in 3-D of each scenario using SCORES3D for a synthetic
 - a. USS imbibition experiment with 2 bump floods
 - b. Multispeed Centrifuge imbibition experiment, with 6 speeds
6. Data analysis was conducted
 - a. Analytically - JBN [1] on selected scenarios to obtain an indication of the effect of V on the relative permeabilities.
 - b. By interpretation-by-simulation - history matching using the newly developed numerical tool AutoSCORES to obtain relative permeabilities and P_c .

7. A rigorous statistical analysis of the results has been carried out, using data sets of up to 1000 AutoSCORES runs (thus simulating up to 1000 laboratory measurements for a single synthetic plug). In this way cut-off values for V could be identified beyond which relative permeability data are significantly different from the perfectly homogeneous base case.

Table 1. Corey parameters used for the scenario runs

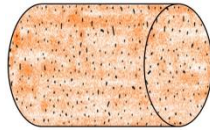
Swc	Sor	krwor	krowc	nw	no
0.1	0.2	0.3	1.0	5	3

3 Details of scenarios

More than 70 synthetic scenarios have been investigated in this study. An overview is presented in Tables 2a-2g.

The base porosity (ϕ_1) was set to 0.17, and the base permeability was set to 10 mD. Scenario A0 represents a perfectly homogeneous plug. The SCAL simulator SCORES3D has been fitted with a random number generator [11], to generate normally distributed porosities assigned randomly to each grid block. The absolute permeability in each grid block was then derived from a standard exponential correlation [6], while the capillary pressure in each grid block was derived through a Leverett-J correlation [6].

Table 2a. Characteristics of heterogeneity scenarios: no layers, σ_ϕ : standard deviation of porosity distribution; ϕ_{eff} : effective (average) porosity; K_{eff} : effective permeability; V: heterogeneity number [6]. Note: $9.87 \times 10^{-15} \text{ m}^2 = 10 \text{ mD}$.



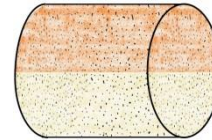
Id	σ_ϕ	ϕ_2	ϕ_{eff}	K_{eff} (10^{-15} m^2)	V
B1	.001	-	.17	9.87	.02
B2	.01	-	.17	9.76	.21
B3	.02	-	.17	9.52	.44
B33	.03	-	.17	9.20	.69
B34	.04	-	.17	8.84	.99
B4	.05	-	.17	8.47	1.4

Table 2b. Characteristics of heterogeneity scenarios: “speckled” plug (see text), σ_ϕ : cut-off factor (see text) for standard deviation of porosity distribution; ϕ_{eff} : effective (average) porosity; K_{eff} : effective permeability; V: heterogeneity number [6]. Note: $9.87 \times 10^{-15} \text{ m}^2 = 10 \text{ mD}$.



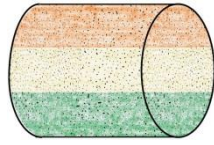
Id	σ_ϕ	ϕ_2	ϕ_{eff}	K_{eff} (10^{-15} m^2)	V
C1	x1	-	.12	2.52	.68
C2	x2	-	.16	8.53	.22
C225	x2.25	-	.17	9.13	.16
C250	x2.5	-	.17	9.51	.11
C275	x2.75	-	.17	9.70	.08
C3	x3	-	.17	9.79	.05

Table 2c. Characteristics of heterogeneity scenarios: 2-layers of equal thickness, σ_ϕ : standard deviation of porosity distribution; ϕ_{eff} : effective (average) porosity; K_{eff} : effective permeability; V: heterogeneity number [6]. Note: $9.87 \times 10^{-15} \text{ m}^2 = 10 \text{ mD}$.



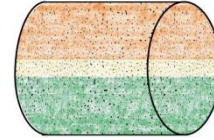
Id	σ_ϕ	ϕ_2	ϕ_{eff}	K_{eff} (10^{-15} m^2)	V
D01	.001	.16	.17	8.73	.11
D1	.001	.15	.16	7.77	.21
D2	.01	.15	.16	7.69	.30
D3	.02	.15	.16	7.50	.49
D4	.05	.15	.16	6.71	1.4
D5	.001	.19	.18	13.0	.21
D6	.01	.19	.18	12.9	.30
D7	.02	.19	.18	12.5	.49
D8	.05	.19	.18	11.2	1.4
D9	.001	.21	.19	17.7	.39
D10	.01	.21	.19	17.5	.45
D11	.02	.21	.19	17.1	.61
D12	.05	.21	.19	15.2	1.5

Table 2d. Characteristics of heterogeneity scenarios: plug with 3-layers of equal thickness, ϕ_2 : porosity of middle layer; σ_ϕ : standard deviation of porosity distribution; ϕ_{eff} : effective (average) porosity; K_{eff} : effective permeability; V : heterogeneity number [6]. Note: $9.87 \times 10^{-15} \text{ m}^2 = 10 \text{ mD}$.



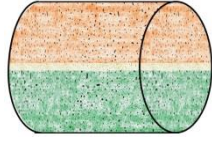
Id	σ_ϕ	ϕ_2	ϕ_{eff}	K_{eff} (10^{-15} m^2)	V
E01	.001	.16	.17	9.12	.10
E1	.001	.15	.16	8.47	.20
E2	.01	.15	.16	8.38	.29
E3	.02	.15	.16	8.19	.48
E4	.05	.15	.16	7.34	1.4
E5	.001	.19	.18	11.9	.21
E6	.01	.19	.18	11.8	.31
E7	.02	.19	.18	11.5	.50
E8	.05	.19	.18	10.4	1.4
E9	.001	.21	.19	14.9	.42
E10	.01	.21	.19	14.8	.48
E11	.02	.21	.19	14.4	.64
E12	.05	.21	.19	13.0	1.6

Table 2e. Characteristics of heterogeneity scenarios: plug with 3-layers, middle layer with ϕ_2 of about 4 mm thickness, σ_ϕ : standard deviation of porosity distribution; ϕ_{eff} : effective (average) porosity; K_{eff} : effective permeability; V : heterogeneity number [6]. Note: $9.87 \times 10^{-15} \text{ m}^2 = 10 \text{ mD}$. For layer with $\phi_2 = 0$, $\sigma_{\phi_2} = 0$.



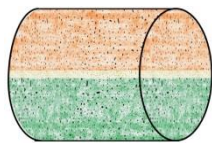
Id	σ_ϕ	ϕ_2	ϕ_{eff}	K_{eff} (10^{-15} m^2)	V
F1	.001	.15	.17	9.50	.12
F2	.01	.15	.17	9.40	.24
F3	.02	.15	.17	9.19	.46
F4	.05	.15	.17	8.27	1.4
F5	.001	.19	.17	10.5	.16
F6	.01	.19	.17	10.4	.27
F7	.02	.19	.17	10.1	.47
F8	.05	.19	.17	9.09	1.4
F9	.001	.21	.18	11.3	.37
F10	.01	.21	.18	11.2	.43
F11	.02	.21	.17	10.9	.59
F12	.02	.21	.17	9.82	1.5
F13	.001	.0	.15	8.76	.37
F14	.01	.0	.15	8.67	.43
F15	.02	.0	.15	8.47	.59
F16	.05	.0	.15	7.60	1.5

Table 2f. Characteristics of heterogeneity scenarios: plug with 3-layers, middle layer with ϕ_2 of about 2 mm thickness, σ_ϕ : standard deviation of porosity distribution; ϕ_{eff} : effective (average) porosity; K_{eff} : effective permeability; V : heterogeneity number [6]. Note: $9.87 \times 10^{-15} \text{ m}^2 = 10 \text{ mD}$. For layer with $\phi_2 = 0$ and with $\phi_2 = 0.5$: $\sigma_{\phi_2} = 0$.



Id	σ_ϕ	ϕ_2	ϕ_{eff}	K_{eff} (10^{-15} m^2)	V
G1	.001	.15	.17	9.70	.09
G2	.01	.15	.17	9.60	.23
G3	.02	.15	.17	9.37	.45
G4	.05	.15	.17	8.38	1.4
G5	.001	.19	.17	10.2	.12
G6	.01	.19	.17	10.1	.25
G7	.02	.19	.17	9.83	.46
G8	.05	.19	.17	8.79	1.4
G9	.001	.21	.17	10.6	.29
G10	.01	.21	.17	10.5	.36
G11	.02	.21	.17	10.2	.54
G12	.02	.21	.17	9.15	1.4
G13	.001	.0	.16	9.34	.25
G14	.01	.0	.16	9.25	.33
G15	.02	.0	.16	9.02	.52
G16	.05	.0	.16	8.03	1.4
G170	.001	.5	.19	49.6	3.9

Table 2g. Characteristics of heterogeneity scenarios: plug with 3-layers, middle layer with ϕ_2 of about 0.3 mm thickness, σ_ϕ : standard deviation of porosity distribution; $\sigma_{\phi_2} = 0$; ϕ_{eff} : effective (average) porosity; K_{eff} : effective permeability; V : heterogeneity number [5]. Note: $9.87 \times 10^{-15} \text{ m}^2 = 10 \text{ mD}$.



Id	σ_ϕ	ϕ_2	ϕ_{eff}	K_{eff} (10^{-15} m^2)	V
G17	.001	.5	.17	38.1	10
G18	.001	.6	.17	53.1	11
G19	.001	.7	.17	56.1	11
G20	.001	.8	.18	56.5	11

The B scenarios (Table 2a) represent heterogeneous core plugs without any layering, but with porosity normally distributed over the grid blocks (and therefore permeability follows a log-normal distribution [6]) throughout the whole plug. The standard deviation of the porosity distribution was varied as indicated.

The settings for the standard deviation for the C scenarios (Table 2b) are shown as multipliers for σ_ϕ . SCORES3D uses this information to adjust any porosity that would be selected by the random number generator to be outside e.g. 2σ , back to the value of 0.001, while setting all other porosity values to a flat value of ϕ_1 (0.17). For that reason, the C scenarios are called “speckled”, because this is how these would show up in a CT image: many white spots representing impermeable spots. This is seen in the laboratory e.g. if disseminated pyrite or glauconite nodules are present.

D scenarios (Table 2c) have two layers of equal thickness into the direction of flow, the porosity of the second layer was set to ϕ_2 . E scenarios (Table 2d) have three layers of equal thickness, with the porosity of the middle layer set to ϕ_2 and for the third layer set equal to ϕ_1 . Scenarios F (Table 2e) and G (Table 2f) have a thin middle layer. Scenarios F13 through F16 and G13 through G16 have a non-permeable layer into the direction of flow.

Scenarios G170 (Table 2f), G17 to G20 (Table 2g) represent a core plug with a thin or very thin open fracture in the flow direction. Permeability in the fracture was set to 1000 times the base permeability.

The heterogeneity number V is calculated internally in SCORES3D and listed in Tables 2a-2g as well.

4 AutoSCORES

As discussed above, we have developed AutoSCORES to conduct automatic history matching of SCAL laboratory experiments. AutoSCORES currently allows history matching of SS (Steady-State), USS, Centrifuge and Porous Plate experiments, simultaneously or in isolation. As part of AutoSCORES, the experiments (real or synthetic) are simulated with SCORES [7,8] in one dimension (SCORES1D) to account for the interference between capillary pressure and relative permeabilities.

History matching is conducted by searching for the least square deviation between experimentally measured production data and production data generated by SCORES1D, through varying the input relative permeability and capillary pressure. The Levenberg-Marquardt (LM) method [11] is used as search algorithm, similar as used by SENDRA [12, 13] or Cydar [14].

Input relative permeabilities are defined in a 6-parameter Corey formulation (see Eqs. 2 and 3): S_{wc} , S_{or} , kr_{wor} , k_{rowc} , n_o and n_w . The relative permeabilities are then submitted as tables to SCORES1D. The saturation tables are refined near low relative permeability.

The input capillary pressure is defined through a specially constructed 11 point table. We tested first LET [15] and other formulations [16] for capillary pressure but these proved to have insufficient flexibility to deal with very sharply bending imbibition capillary pressure curves as seen in the laboratory. Within SCORES1D all saturation tables are interpolated by monotonous cubic spline functions [17].

The capillary pressure table is generated between S_{wc} and $1-S_{or}$, so it has two points in common with the Corey relative permeability formulation. This results in AutoSCORES searching for an optimal $6+9=15$ component “state vector” [11; Chapter 15.4] delivering a match between the experimental production curves and the production curves generated by SCORES1D.

4.1 Brief overview of the design of AutoSCORES

The LM method can be seen as a special strategy in a Newton-Raphson (NR) process that seeks the zero value of a function [11]. NR requires the calculation of the derivative of the function. For the case at hand, the function is constructed comparing a selection of points on the production curves generated by SCORES1D, against a corresponding set of points on the experimental (or synthetic as the case may be) production curves perturbed with a certain noise level [11; Chapter 15.1]. This selection is used to construct a so-called Chi-square function. The LM method then searches for the minimum Chi-squared value while varying the state-vector. Generally, the selection of points consists of several 1000’s of data points N_{data} (automatically selected within AutoSCORES).

The derivative consists of 15 partial derivatives, one for each component in the state vector. So-called 2-sided derivatives are used to increase stability of the search algorithm.

For our study we conducted history matching of a USS and a multi-speed centrifuge (numerical) experiment

simultaneously, requiring a base run and 30 “derivative” runs per iteration, per experiment, so in total 62 runs per iteration. The LM method usually converged after 5 to 10 iterations.

A major advantage of this approach is that the minimum Chi-square has a known expectation value: this value is equal to N_{data} [11; Chapter 5.1]. Searching for a minimum value of a function of a multicomponent state-vector can never be guaranteed to deliver the correct answer. A local minimum in the multi-dimensional space can be found instead. However, at least wrong, way too large or too small, values found after convergence can be rejected, based on the expectation value and based on the known standard deviation of the Chi-square function. AutoSCORES rejects results deviating more than 4 standard deviations, corresponding to a probability of less than 0.006% for being a correct result. After testing, the convergence tolerance for Chi-square was set to 0.001, normalised to N_{data} . For a tighter tolerance setting, the distributions of the extracted Corey parameters did not change significantly from the values found with 0.001.

As an example, we present in Fig. 1 a typical matched production profile for a multispeed centrifuge run as used in our study. The data of the (numeric) experiment include the noise added. The above mentioned convergence and tolerance settings clearly prove to be effective.

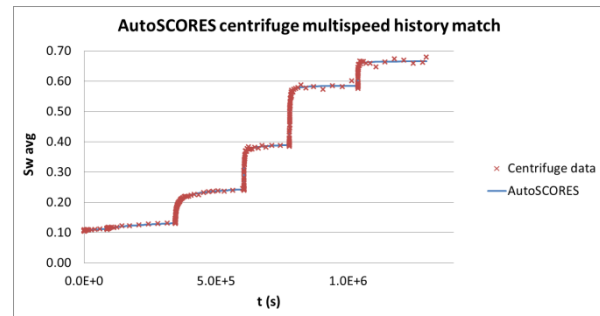


Fig. 1. Example of AutoSCORES matching a production profile of a multi-speed imbibition centrifuge experiment. Average water saturation is plotted as a function of time (s).

In view of the large amount of AutoSCORES runs required for this study, dedicated hardware was set-up with two DELL R-815 32-core servers, with 128 GB memory each, which allows parallel processing of all 62 runs per iteration. This brought about a significant reduction in run time. AutoSCORES was written in C++ and was run on a Windows platform that controlled the two servers for parallel processing. We found that the servers were not fully loaded during the LM iterations. This allowed us to run up to four Windows machines with AutoSCORES, in parallel, feeding the servers and we obtained thus a further reduction in turn-around time in this research project. AutoSCORES is designed to run also in sequential mode on a single Windows platform in case no massive amount of history matching is required.

5 Statistical Analysis

First, the performance of the tools (SCORES3D and AutoSCORES) developed in this study has been

evaluated through statistical analysis. A short but excellent introduction to statistical data analysis can be found in Numerical Recipes [11].

A large number of simulations confirmed that SCORES3D produces stochastically distributed heterogeneities that we can be confident to follow a normal distribution which means that parametric statistics [18] can be used in data analysis. Subsequently, a Chi-squared (goodness of fit) test [11; Chapter 14.3] was used to test whether an observed distribution of parameters extracted by AutoSCORES, such as Corey parameters, deviated from a normal distribution having the same mean and standard deviation.

A students t-test [11; Chapter 14.2] was used to test for significant differences between the heterogeneity scenarios (Tables 2a-2g) and a corresponding isotropic homogeneous base case scenario, see the example in the Section below. An F-test was conducted [11; Chapter 14.2] to check for equal variances before the t-statistic could be calculated. The significance of the calculated statistics was evaluated against tables of significant test levels of the respective probability density distributions [19].

With the performance of SCORES3D and AutoSCORES proven statistically reliable, we proceeded to use the tools to study the impact of heterogeneity on SCAL parameters.

5.1 Analysing the impact of heterogeneity

Ignoring the effect of the V cut-off would allow the plug to be part of a SCAL program and its relative permeabilities and Pc to be extracted. The impact of the actual heterogeneities of a certain scenario Z therefore is best judged by comparing the relative permeabilities extracted for Z with the relative permeabilities extracted for a corresponding homogeneous base case A0_Z.

A0_Z is a SCORES3D run with $V=0$, and permeability and porosity set equal to the effective permeability and porosity of scenario Z^a.

As an example of how we investigated the heterogeneity cut-off values, we discuss here the B-scenarios, representing a single layer with random scatter in ϕ (Table 2a). Each scenario was tested against the corresponding base case scenarios labelled A0_BX. For instance, consider heterogeneity scenario B1. According to Table 2a, the average porosity and permeability of B1 are 0.17 and $9.87 \times 10^{-15} \text{ m}^2$ respectively. Therefore a homogeneous run labelled A0_B1 was executed with SCORES3D with all grid blocks set to a single porosity and permeability value of 0.17 and $9.87 \times 10^{-15} \text{ m}^2$ respectively. The results from the A0_B1 run would have been observed in the laboratory if the core plug indeed would have been perfectly homogeneous. Any differences

^a Effective permeability of the synthetic heterogeneous sample was determined either by a separate 3-D simulation of brine injection into a fully brine saturated sample, or from the pressure drop in the simulated 3-D USS experiment at early

between interpretation-by-simulation of A0_B1 and B1 therefore are directly the result of B1 being heterogeneous. In Table 3 we present results found for the Corey nw parameter for all B scenarios.

While testing AutoSCORES, a number of scenarios have been run with N different seeds for the noise added to the production data (see Section 4.1), with N set to 10, 100 and even 1000 for selected cases. However, in a laboratory environment a realistic number of SCAL samples is likely to be much lower, and a case for N=3 has been settled for in this example, i.e. small sample statistics shall be used in analysis.

First a so-called null hypothesis H0 of "no difference between the average nw found for BX and A0_BX" is formulated and tested using a t-test (Table 3). The t-test considers the difference between two averages (X1 and X2), using the standard deviations (s1 and s2) and the number N of simulations in the SCAL experiment. The calculated t-value t_{calc} is then compared against the critical test value t_{crit} (at a 5% or 1% test level) found from a table of the t probability density distribution [19]. If we find $t_{\text{calc}} \leq t_{\text{crit}}$ then H0 stands and we accept there is no significant difference between the two scenarios. For $t_{\text{calc}} > t_{\text{crit}}$, H0 is rejected and we can be more than 95% or 99% sure they are different.

Consider scenario B4 vs. A0_B4: the calculated $t=8.07$ is greater than the 5% and 1% test levels having critical $t_{95}=2.78$ and $t_{99}=4.60$, i.e. we can be more than 99% sure that B4 is different from the perfectly homogeneous A0_B4 scenario. However, the remaining B-scenarios with the test levels we have decided for (5% and 1%), are not seen as significantly different from the equivalent perfect homogeneous scenario even for a coefficient of variation V close to 1. This may look as a surprising result but is closely related to the t-probability distribution and the calculation of the t-statistic. Both are very sensitive to the number of samples N if N is small, as shown in Table 4.

In effect, with a larger number of samples, the accuracy improves with which the mean value of e.g. nw is determined. At improved accuracy, a statistical analysis will then detect reliably a smaller difference between nw of a heterogeneous plug and a homogeneous one [11; Chapter 14.2]. In the ideal case of 100 or more plugs, the t-distribution approaches the normal distribution having the minimal critical $t_{95}=1.96$ and $t_{99}=2.58$ and thus the maximum strength in testing the significance of difference between means.

From the scenarios listed in Tables 3 and 4 it is clear that an increase in the number of samples from 3 to 10 can reduce the cut-off for V to around 0.5. This means that only the three scenarios B1-B3 in Table 4 would qualify as homogeneous in SCAL measurements if 10 samples were available.

times, given the known (inputted) end point of the oil relative permeability at initial water saturation. Both methods agreed within 0.25%.

Table 3. Statistical test of the difference between Corey nw's calculated from different BX scenarios vs. their corresponding base case A0_BX at N=3. When the null hypothesis is 'True' the result is said to be non-significant (non-S), when it is 'False' the result is significant (S), i.e. the 2 scenarios are different.

Statistic →	X_1	X_2	s_1	s_2	df	$t_{calc.}$	H_0	Result	H_0	Result	V	
Scenario ID ↓							[5%]	[5%]	[1%]	[1%]		
B1 vs A0_B1	4.967	4.945	0.063	0.056	4	0.438	True	non-S	True	non-S	0.021	
B2 vs A0_B2	4.933	4.954	0.062	0.062	4	0.410	True	non-S	True	non-S	0.21	
B3 vs A0_B3	4.950	5.017	0.065	0.094	4	1.018	True	non-S	True	non-S	0.44	
B33 vs A0_B33	4.872	5.061	0.098	0.140	4	1.917	True	non-S	True	non-S	0.69	
B34 vs A0_B34	4.916	5.126	0.067	0.172	4	1.972	True	non-S	True	non-S	0.99	
B4 vs A0_B4	4.945	5.526	0.066	0.105	4	8.07	False	S	False	S	1.37	
Conditions :	$N_1=N_2=3$				$t_{95} =$	2.78			$t_{99} =$	4.60	<i>df=deg. of freedom</i>	
	X_1 : Avg A0_BX				X_2 : Avg BX			s_1 : Stdev A0_BX			s_2 : Stdev BX	

Table 4. Statistical test of difference between Corey nw's calculated from different B scenarios vs. their base case A0_BX at N=10. Compare with the cut-off value of V for N=3 in Table 3 above.

Statistic →	X_1	X_2	s_1	s_2	df	$t_{calc.}$	H_0	Result	H_0	Result	V	
Scenario ID ↓							[5%]	[5%]	[1%]	[1%]		
B1 vs A0_B1	4.967	4.945	0.063	0.056	18	0.799	True	non-S	True	non-S	0.021	
B2 vs A0_B2	4.933	4.954	0.062	0.062	18	0.748	True	non-S	True	non-S	0.21	
B3 vs A0_B3	4.950	5.017	0.065	0.094	18	1.859	True	non-S	True	non-S	0.44	
B33 vs A0_B33	4.872	5.061	0.098	0.140	18	3.50	False	S	False	S	0.69	
B34 vs A0_B34	4.916	5.126	0.067	0.172	18	3.60	False	S	False	S	0.99	
B4 vs A0_B4	4.945	5.526	0.066	0.105	18	14.7	False	S	False	S	1.37	
Conditions :	$N_1=N_2=10$				$t_{95} =$	2.10			$t_{99} =$	2.88	<i>df=deg. of freedom</i>	
	X_1 : Avg A0_BX				X_2 : Avg BX			s_1 : Stdev A0_BX			s_2 : Stdev BX	

Table 5. Cut-off values for V , per scenario, established for a small number of samples ($N \approx 3$). For plugs with V below the cut-off, heterogeneities will have a non-significant impact on the relative permeabilities extracted through interpretation-by-simulation of the SCAL experiments.

Scenario	Short description	V cut-off
B	stochastically distributed Gaussian porosity distribution	0.9
C	“speckled” (see Section 3) core plug	0.2
D	dual layer in flow direction	0.15
E	three layers in flow direction, equal thickness	0.1
F	three layers in flow direction, middle layer thickness ≈ 4 mm	0.1
G [G1-G8]	three layers, middle layer ≈ 2 mm	0.8
G [G9-G12]	three layers, middle layer ≈ 2 mm, and of significantly higher porosity	0.1
G [G13-G15]	three layers, middle layer ≈ 2 mm, and impermeable	0.4
open fracture	one or more open fractures in flow direction	0

6 Results on synthetic data

A detailed analysis has been conducted on the 70+ scenarios listed in Table 2a-2g. Through interpolation and extrapolation of V versus t_{calc} , cut-off values were defined in a straightforward manner for scenarios B, C, D and G and listed in Table 5.

The results for scenarios E and F proved to be more difficult to interpret. We noticed e.g. that scenarios E1, E2 and E3 showed False, while E4 showed True, i.e. E4 is not significantly different from a homogeneous case with the same effective permeability and porosity, while E1-3 are different. A similar situation occurred for F1-4. This behaviour is due to the fact that with increasing σ_ϕ , the E and F scenarios in the 1-4 sequence are changing character from a clearly layered system into a more evenly stochastically distributed porosity/permeability distribution. In other words: changing from E1 to E4, the core plug looks more and more like a B3 or B4 scenario. As shown in Table 5, the B scenarios have a very high cut-off, meaning that up to $V=0.9$ the samples behave like homogeneous samples. In fact, it will be impossible from CT images to make a distinction between an E4 or F4 scenario and a B4 scenario. Scenarios can only be used in determining a cut-off value for V if these can be recognised in the images in the first place.

So, we interpret the results for the E and F scenarios as follows: if a layering is visible in the CT images, the cut-off is 0.1, both for E and F scenarios.

Note that E and F scenarios represent three-layered plugs of which the middle layer has a thickness of several mm. The middle layer in the G scenarios has a thickness of only 2 mm (G1-G15). Our results indicate that for G1-G8, the cut-off is 0.8. In fact, G1 to G8, with only a small porosity difference between the middle layer and layers 1 and 3, behave similar to the B scenarios. However, if the middle layer has a porosity of at least 0.04 larger than layers 1 and 3, the cut-off is 0.1 (G9-G12).

For thin layers with no porosity, as modelled by G13-G15, we see a cut-off of 0.4.

If the middle layer is an open fracture (G170 and G17-G20), the cut-off is basically zero: no plug with that

scenario will behave like an unfractured, homogeneous plug.

Finally, we investigated a limited number of sensitivities. We checked how the cut-off values would change for the B and G13-G15 scenarios if absolute permeability was set to 1 mD, 100 mD and 1000 mD, or if the capillary pressure was changed to a much sharply bent imbibition curve, i.e. an imbibition curve showing hardly any spontaneous water imbibition. We found no significant difference with the cut-off values seen before.

We have not tested sensitivity with respect to the chosen Corey parameters. At first glance, a change of e.g. a water Corey exponent from 5 as used in this study to 3 would bring about a higher water mobility and therefore could accelerate break-through. However, since in our scenarios, all layers have the same Corey parameters, the overall net effect is probably of second order: all layers would see similar acceleration of break-through, cancelling a net effect.

7 Laboratory experiments

In support of conclusions derived from synthetic data, USS laboratory experiments were conducted with gas-brine in drainage mode. Out of a set of 12 Oberkirchener (OBKN) sandstone samples, three samples were selected (G2, G3 and B2), with a porosity around 0.17 and permeability of about 10 mD. CT DICOM-images were analysed and we found that the heterogeneity numbers V for all three samples were around 0.26. Sample B2 (Fig. 2) had two stylolites filled with higher density material, but still had overall porosity, absolute permeability and V similar to G2 and G3. Samples G2 and G3 had no stylolites or other distinct features observable by the naked eye or in CT images and therefore fall into a class B scenario. Sample B2 falls into a class G13 scenario. According to the results presented in Section 6, SCAL parameters extracted by AutoSCORES should deliver similar results for these three samples, given $V \approx 0.26$.

The three samples were measured in UnSteady-State mode, at constant pressure drop as is customary for gas-

brine drainage experiments [20]. Gas was equilibrated with brine at injection pressure by bubbling the gas through a PanTerra-designed humidifier mounted in-line. The humidifier consists of two cylinders, partially brine filled that are connected at the bottom. Gas is injected at the top of one cylinder and escapes at the top of the other. Residence time of the gas in the brine is in the order of 20 to 2 seconds, dependent on the flow rate. Back pressure was set fixed at 190 psi, and initial pressure drop was set to 20 psi. This value was determined using SCORES as a design tool. In design mode, one uses guestimated relative permeabilities and capillary pressure. Relative permeabilities were chosen as typical for drainage in a water-wet plug (the OBKN plugs had been soxhlet-cleaned before the experiments) and the drainage capillary pressure was chosen similar to the curve found in OBKN centrifuge drainage experiments on other OBKN plugs several years ago.

The experiments were run into a gas-brine separator that had been mounted upstream of the back-pressure regulator, so that this regulator only dealt with a gas flow. Production data were automatically recorded with a data logger connected to an electronic balance collecting the cumulative water production and to electronic gas flow sensors. Once that the gas-cut reached 99.95% (vol/vol, at standard conditions), the differential pressure was increased to 40 psi and subsequently to 100 psi, as bump floods, in order to reduce the capillary end-effects. The cumulative water production and gas flow rate of the USS experiments in conjunction with the production curve from the primary drainage centrifuge experiment mentioned before, were history matched with AutoSCORES.

The centrifuge data were brought-in to constrain the results of AutoSCORES: i.e. the Corey parameters of relative permeability, together with an assessment of the drainage capillary pressure. Using 10 to 100 different seeds for the applied noise level in AutoSCORES, statistics were obtained for all parameters to allow assessment of similarity (the H0 hypothesis as mentioned in Section 5) between the three plugs. Tables 6 and 7 summarise the results for the Corey parameters.

Note that these experiments were conducted in primary drainage, so S_{rg} does not play a role. Rather a percolation threshold exists that we assumed fixed at 0.02. For the same reason the Corey parameter kr_{wgr} was fixed at 0.98.

Except for kr_{gwc} , plugs B2, G2 and G3 are characterised by the same Corey parameters with a confidence level of 99%, despite the presence of impermeable stylolites in plug B2. This result is obtained using small number of samples statistics ($N=3$) as above. Analysis shows that in order to see a possible difference at confidence levels 95% and 99%, one would need some 10 plugs or more.

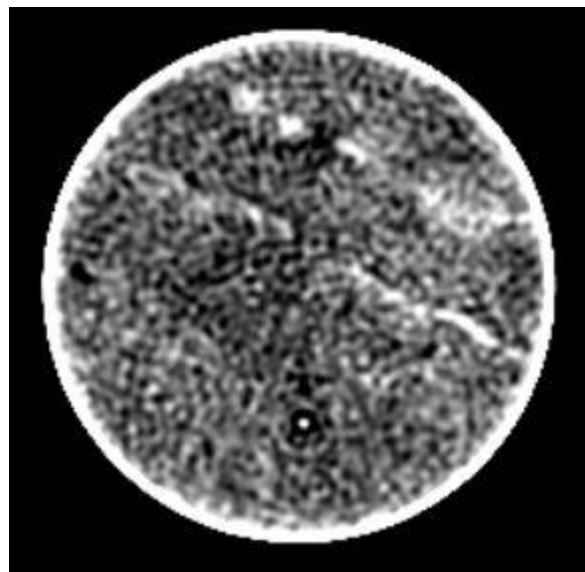


Fig. 2. Sample B2 with two stylolites visible, and a CT tomogram of B2. The stylolites appear as white streaks in CT, because high densities are translated into white pixels.

Table 6. nw, ng, krgwc, Swc results on OBKN G2 and G3, conditions similar to Table 3. σ : standard deviation.

Statistic : →	Avg. G2	Avg. G3	$\sigma(G2)$	$\sigma(G3)$	df	$t_{calc.}$	H_0	Result	H_0	Result
OBKN G2 vs G3: ↓							[5%]	[5%]	[1%]	[1%]
nw	4.19	3.85	0.23	0.17	4	2.04	True	non-S	True	non-S
ng	2.69	2.95	0.23	0.15	4	1.66	True	non-S	True	non-S
krgwc	0.52	0.58	0.03	0.03	4	2.52	True	non-S	True	non-S
Swc	0.05	0.05	0.02	0.01	4	0.04	True	non-S	True	non-S

Table 7. nw, ng, krgwc, Swc results on OBKN B2 and G2, conditions similar to Table 3. σ : standard deviation.

Statistic : →	Avg. B2	Avg. G2	$\sigma(B2)$	$\sigma(G2)$	df	$t_{calc.}$	H_0	Result	H_0	Result
OBKN B2 vs G2: ↓							[5%]	[5%]	[1%]	[1%]
nw	4.26	4.19	0.30	0.23	4	0.32	True	non-S	True	non-S
ng	2.44	2.69	0.18	0.23	4	1.41	True	non-S	True	non-S
krgwc	0.36	0.52	0.03	0.03	4	6.34	False	S	False	S
Swc	0.06	0.05	0.03	0.02	4	0.65	True	non-S	True	non-S

Krgwc is shown to be significantly different between B2 and the two other plugs. This parameter is derived mainly from the production data at the end of the experiment, i.e. from the last bump flood. The experiment on the G2 and G3 plugs were terminated earlier than on the B2 plug where we had additional focus on late time behaviour. This may well have caused salt precipitation in plug B2 to be more significant than in the G2 and G3 experiments. B2 showed a reduction in absolute permeability after the experiment of about 25% while G2 and G3 showed a reduction of only 5%. Note that the reduction in permeability is similar to the reduction observed for krgwc. We do not know when the reduction in permeability of B2 occurred, but if it indeed would have been during the later phase of the experiment, later time data would have been affected most. As a result, krgwc would then be strongly affected: AutoSCORES was not set to use the absolute permeability as an adjustable parameter, so a reduction in the lab of the absolute permeability translates into a correspondingly lower value for krgwc. If one would be allowed to correct for this effect, an adjusted value for krgwc of B2 would bring the H_0 at the 5% level to True, i.e. no significant difference in krgwc can be observed anymore between B2 and the two other samples.

Finally, it is of interest to note that the analytical JBN calculation on B2, G2 and G3 showed $ng \approx 2$, $nw \approx 3$ and $Swc \approx 0.2$. Moreover, Dean-Stark extraction on the plugs after the experiments showed average final water saturations in the order of 0.2. This demonstrates how end-effects, even at high differential pressure in a gas-brine drainage experiment may still dominate the results and that history matching the production data makes a real difference in interpreted results.

8 Conclusions

A cut-off value for the heterogeneity value V of a core sample represents the value beyond which flow parameters measured in SCAL experiments will be significantly affected by heterogeneity. When that happens, the plug needs to be discarded because no reliable SCAL data can be measured on that core plug. Using such data would compromise simulations on the field scale with possibly serious effects on development plans.

In summary we have:

- Cut-off values for the heterogeneity number V have been defined now for many scenarios as these come about in laboratory practice.
- The cut-off value for V is strongly dependent on the heterogeneity scenario seen in CT images of plug.
- Layering in a plug strongly reduces the cut-off value for V .
- The recommended work flow is to conduct RCA and CT-scanning and establish the heterogeneity number V for all candidate plugs. Based on the observed heterogeneity scenario, the cut-offs presented in Table 5 can then be used to select the plugs that have V below the cut-off value.
- Cut-off values for V are dependent on the number of plugs available for a study. This is caused by the fact that if 10 or more plugs per flow unit are used, the critical test value for the evaluation of the student-t analysis changes substantially from the value used if only 3 samples are available.
- The first laboratory experiments to test the results derived for the synthetic plugs were promising.

A core plug with visible stylolites showed flow parameters similar to an unperturbed plug, as predicted by our heterogeneity analysis.

- AutoSCORES allows for history matching multiple experiments simultaneously. All SCAL laboratory experiments can be addressed.

The CT-scans of the OBKN material were made available courtesy of Prof. Pacelli Zitha, TUDelft, and conducted expertly by Mrs. Ellen Meijvogel-de Koning.

We acknowledge the accurate work by Xiangmin Zhang, PanTerra Geoconsultants, who conducted the UnSteady-State experiments.

References

1. E.F. Johnson, D.P. Bossler, V.O. Naumann, "Calculation of relative permeability from displacement experiments," AIME **216**, 370–372 (1959)
2. G. Hassler, E. Brunner, "Measurement of capillary pressures in small core samples", Trans. AIME **160**, 114-123 (1945)
3. A. Sylte, T. Manseth, J. Mykkeltveit, J.E. Nordtvedt, "Relative permeability and capillary pressure: effects of rock heterogeneity", SCA-9808 (1998)
4. A. Zweers, W. Scherpenisse, K. Wit, J. Maas, "Relative permeability measurements on heterogeneous samples. A pragmatic approach", SCA-9909 (1999)
5. D. Fenwick, N. Doerler, R. Lenormand, "The effect of heterogeneity on unsteady-state displacements", SCA2000-30 (2000)
6. J.G. Maas, A. Hebing, "Quantitative X-ray CT for SCAL plug homogeneity assessment", SCA 2013-004 (2013)
7. J.G. Maas, B. Flemisch, A. Hebing, "Open source simulator DuMux available for SCAL data interpretation", SCA 2011-08 (2011)
8. R. Lenormand, K. Lorentzen, J. G. Maas and D. Ruth, "Comparison of four numerical simulators for SCAL experiments", SCA 2016-06 (2016)
9. J. Reed, J.G. Maas, "Review of the intercept method for relative permeability correction using a variety of case study data", SCA 2018-030 (2018)
10. R. Gupta, D. Maloney, "Intercept Method – A novel technique to correct steady-state relative permeability data for capillary end-effect", SPE Reservoir Evaluation & Engineering, SPE 171797, doi:10.2118/171797-MS (2014)
11. W.H. Preuss, B.P. Flannery, S.A. Teukolsky, W.T. Vetterling, *Numerical Recipes in C++, The Art of Scientific Computing*, 2nd Edition, Cambridge University Press, Cambridge (2002). See also <http://www.numerical.recipes>
12. E. Ebeltoft, A. Sylte, E.B. Petersen Jr., "Simultaneous determination of relative permeability and capillary pressure from several types of experiments", SCA2004-17 (2004)
13. A.T. Watson, P.C. Richmond, P.D. Kerig, T.M. Tao, "A regression-based method for estimating relative permeabilities from displacement experiments", SPE Reservoir Engineering, Aug. 1988, p 953 (1998)
14. CYDAR user manual, see <http://www.cydarex.fr>
15. F. Lomeland, E. Ebeltoft, "A new versatile capillary pressure correlation", SCA2008-08
16. D. Loeve, F. Wilschut, R.H. Hanea, J.G. Maas, P.M.E. van Hoof, P.J. van den Hoek, S.G. Douma, J.F.M. Van Doren, "Simultaneous determination of relative permeability and capillary pressure curves by assisted history matching several SCAL experiments", SCA2011-35 (2011)
17. F.N. Fritsch, R.E. Carlson, "Monotone piecewise cubic interpolation", SIAM J. Numer. Anal. **17(2)**, 238-246 (1980)
18. R.A. Fisher, *Statistical Methods for Research Workers*, Edinburgh, Oliver & Boyd (1962)
19. R.A. Fisher, F. Yates, *Statistical tables for biological, agricultural and medical research*, London, Oliver & Boyd (1963)
20. Potter, G. and G. Lyle, "Measuring unsteady-state gas displacing liquid relative permeability of high permeability samples", SCA 9419 (1994)